

Measurement of $\sigma \cdot B(W \rightarrow e\nu)$ and $\sigma \cdot B(Z^0 \rightarrow e^+e^-)$ in $p\bar{p}$ collisions at $\sqrt{s} = 1.8$ TeV

F. Abe,¹³ M. G. Albrow,⁷ S. R. Amendolia,²³ D. Amidei,¹⁶ J. Antos,²⁸ C. Anway-Wiese,⁴ G. Apollinari,²⁶ H. Areti,⁷ M. Atac,⁷ P. Auchincloss,²⁵ F. Azfar,²¹ P. Azzi,²⁰ N. Bacchetta,²⁰ W. Badgett,¹⁶ M. W. Bailey,¹⁸ J. Bao,³⁵ P. de Barbaro,²⁵ A. Barbaro-Galtieri,¹⁴ V. E. Barnes,²⁴ B. A. Barnett,¹² P. Bartalini,²³ G. Bauer,¹⁵ T. Baumann,⁹ F. Bedeschi,²³ S. Behrends,³ S. Belforte,²³ G. Bellettini,²³ J. Bellinger,³⁴ D. Benjamin,³¹ J. Benlloch,¹⁵ J. Bensinger,³ D. Benton,²¹ A. Beretvas,⁷ J. P. Berge,⁷ S. Bertolucci,⁸ A. Bhatti,²⁶ K. Biery,¹¹ M. Binkley,⁷ F. Bird,²⁹ D. Bisello,²⁰ R. E. Blair,¹ C. Blocker,³ A. Bodek,²⁵ W. Bokhari,¹⁵ V. Bolognesi,²³ D. Bortoletto,²⁴ C. Boswell,¹² T. Boulos,¹⁴ G. Brandenburg,⁹ C. Bromberg,¹⁷ E. Buckley-Geer,⁷ H. S. Budd,²⁵ K. Burkett,¹⁶ G. Busetto,²⁰ A. Byon-Wagner,⁷ K. L. Byrum,¹ J. Cammerata,¹² C. Campagnari,⁷ M. Campbell,¹⁶ A. Caner,⁷ W. Carithers,¹⁴ D. Carlsmith,³⁴ A. Castro,²⁰ Y. Cen,²¹ F. Cervelli,²³ H. Y. Chao,²⁸ J. Chapman,¹⁶ M.-T. Cheng,²⁸ G. Chiarelli,²³ T. Chikamatsu,³² C. N. Chiou,²⁸ L. Christofek,¹⁰ S. Cihangir,⁷ A. G. Clark,²³ M. Cobal,²³ M. Contreras,⁵ J. Conway,²⁷ J. Cooper,⁷ M. Cordelli,⁸ C. Couyoumtzelis,²³ D. Crane,¹ J. D. Cunningham,³ T. Daniels,¹⁵ F. DeJongh,⁷ S. Delchamps,⁷ S. Dell'Agnello,²³ M. Dell'Orso,²³ L. Demortier,²⁶ B. Denby,²³ M. Deninno,² P. F. Derwent,¹⁶ T. Devlin,²⁷ M. Dickson,²⁵ J. R. Dittmann,⁶ S. Donati,²³ R. B. Drucker,¹⁴ A. Dunn,¹⁶ K. Einsweiler,¹⁴ J. E. Elias,⁷ R. Ely,¹⁴ E. Engels, Jr.,²² S. Eno,⁵ D. Errede,¹⁰ S. Errede,¹⁰ Q. Fan,²⁵ B. Farhat,¹⁵ I. Fiori,² B. Flaughner,⁷ G. W. Foster,⁷ M. Franklin,⁹ M. Frautschi,¹⁸ J. Freeman,⁷ J. Friedman,¹⁵ H. Frisch,⁵ A. Fry,²⁹ T. A. Fuess,¹ Y. Fukui,¹³ S. Funaki,³² G. Gagliardi,²³ S. Galeotti,²³ M. Gallinaro,²⁰ A. F. Garfinkel,²⁴ S. Geer,⁷ D. W. Gerdes,¹⁶ P. Giannetti,²³ N. Giokaris,²⁶ P. Giromini,⁸ L. Gladney,²¹ D. Glenzinski,¹² M. Gold,¹⁸ J. Gonzalez,²¹ A. Gordon,⁹ A. T. Goshaw,⁶ K. Goulianos,²⁶ H. Grassmann,⁶ A. Grewal,²¹ L. Groer,²⁷ C. Grosso-Pilcher,⁵ C. Haber,¹⁴ S. R. Hahn,⁷ R. Hamilton,⁹ R. Handler,³⁴ R. M. Hans,³⁵ K. Hara,³² B. Harral,²¹ R. M. Harris,⁷ S. A. Hauger,⁶ J. Hauser,⁴ C. Hawk,²⁷ J. Heinrich,²¹ D. Cronin-Hennessy,⁶ R. Hollebeek,²¹ L. Holloway,¹⁰ A. Hölscher,¹¹ S. Hong,¹⁶ G. Houk,²¹ P. Hu,²² B. T. Huffman,²² R. Hughes,²⁵ P. Hurst,⁹ J. Huston,¹⁷ J. Huth,⁹ J. Hylen,⁷ M. Incagli,²³ J. Incandela,⁷ H. Iso,³² H. Jensen,⁷ C. P. Jessop,⁹ U. Joshi,⁷ R. W. Kadel,¹⁴ E. Kajfasz,^{7a} T. Kamon,³⁰ T. Kaneko,³² D. A. Kardelis,¹⁰ H. Kasha,³⁵ Y. Kato,¹⁹ L. Keeble,⁸ R. D. Kennedy,²⁷ R. Kephart,⁷ P. Kesten,¹⁴ D. Kestenbaum,⁹ R. M. Keup,¹⁰ H. Keutelian,⁷ F. Keyvan,⁴ D. H. Kim,⁷ H. S. Kim,¹¹ S. B. Kim,¹⁶ S. H. Kim,³² Y. K. Kim,¹⁴ L. Kirsch,³ P. Koehn,²⁵ K. Kondo,³² J. Konigsberg,⁹ S. Kopp,⁵ K. Kordas,¹¹ W. Koska,⁷ E. Kovacs,^{7a} W. Kowald,⁶ M. Krasberg,¹⁶ J. Kroll,⁷ M. Kruse,²⁴ S. E. Kuhlmann,¹ E. Kuns,²⁷ A. T. Laasanen,²⁴ N. Labanca,²³ S. Lammel,⁴ J. I. Lamoureux,³ T. LeCompte,¹⁰ S. Leone,²³ J. D. Lewis,⁷ P. Limon,⁷ M. Lindgren,⁴ T. M. Liss,¹⁰ N. Lockyer,²¹ C. Loomis,²⁷ O. Long,²¹ M. Loreti,²⁰ E. H. Low,²¹ J. Lu,³⁰ D. Lucchesi,²³ C. B. Luchini,¹⁰ P. Lukens,⁷ J. Lys,¹⁴ P. Maas,³⁴ K. Maeshima,⁷ A. Maghakian,²⁶ P. Maksimovic,¹⁵ M. Mangano,²³ J. Mansour,¹⁷

M. Mariotti,²⁰ J. P. Marriner,⁷ A. Martin,¹⁰ J. A. J. Matthews,¹⁸ R. Mattingly,¹⁵ P. McIntyre,³⁰ P. Melese,²⁶ A. Menzione,²³ E. Meschi,²³ G. Michail,⁹ S. Mikamo,¹³ M. Miller,⁵ R. Miller,¹⁷ T. Mimashi,³² S. Miscetti,⁸ M. Mishina,¹³ H. Mitsushio,³² S. Miyashita,³² Y. Morita,²³ S. Moulding,²⁶ J. Mueller,²⁷ A. Mukherjee,⁷ T. Muller,⁴ P. Musgrave,¹¹ L. F. Nakae,²⁹ I. Nakano,³² C. Nelson,⁷ D. Neuberger,⁴ C. Newman-Holmes,⁷ L. Nodulman,¹ S. Ogawa,³² S. H. Oh,⁶ K. E. Ohl,³⁵ R. Oishi,³² T. Okusawa,¹⁹ C. Pagliarone,²³ R. Paoletti,²³ V. Papadimitriou,³¹ S. Park,⁷ J. Patrick,⁷ G. Pauletta,²³ M. Paulini,¹⁴ L. Pescara,²⁰ M. D. Peters,¹⁴ T. J. Phillips,⁶ G. Piacentino,² M. Pillai,²⁵ R. Plunkett,⁷ L. Pondrom,³⁴ N. Produit,¹⁴ J. Proudfoot,¹ F. Ptohos,⁹ G. Punzi,²³ K. Ragan,¹¹ F. Rimondi,² L. Ristori,²³ M. Roach-Bellino,³³ W. J. Robertson,⁶ T. Rodrigo,⁷ J. Romano,⁵ L. Rosenson,¹⁵ W. K. Sakumoto,²⁵ D. Saltzberg,⁵ A. Sansoni,⁸ V. Scarpine,³⁰ A. Schindler,¹⁴ P. Schlabach,⁹ E. E. Schmidt,⁷ M. P. Schmidt,³⁵ O. Schneider,¹⁴ G. F. Sciacca,²³ A. Scribano,²³ S. Segler,⁷ S. Seidel,¹⁸ Y. Seiya,³² G. Sganos,¹¹ A. Sgolacchia,² M. Shapiro,¹⁴ N. M. Shaw,²⁴ Q. Shen,²⁴ P. F. Shepard,²² M. Shimojima,³² M. Shochet,⁵ J. Siegrist,²⁹ A. Sill,³¹ P. Sinervo,¹¹ P. Singh,²² J. Skarha,¹² K. Sliwa,³³ D. A. Smith,²³ F. D. Snider,¹² L. Song,⁷ T. Song,¹⁶ J. Spalding,⁷ L. Spiegel,⁷ P. Sphicas,¹⁵ A. Spies,¹² L. Stanco,²⁰ J. Steele,³⁴ A. Stefanini,²³ K. Strahl,¹¹ J. Strait,⁷ D. Stuart,⁷ G. Sullivan,⁵ K. Sumorok,¹⁵ R. L. Swartz, Jr.,¹⁰ T. Takahashi,¹⁹ K. Takikawa,³² F. Tartarelli,²³ W. Taylor,¹¹ P. K. Teng,²⁸ Y. Teramoto,¹⁹ S. Tether,¹⁵ D. Theriot,⁷ J. Thomas,²⁹ T. L. Thomas,¹⁸ R. Thun,¹⁶ M. Timko,³³ P. Tipton,²⁵ A. Titov,²⁶ S. Tkaczyk,⁷ K. Tollefson,²⁵ A. Tollestrup,⁷ J. Tonnison,²⁴ J. F. de Troconiz,⁹ J. Tseng,¹² M. Turcotte,²⁹ N. Turini,²³ N. Uemura,³² F. Ukegawa,²¹ G. Unal,²¹ S. C. van den Brink,²² S. Vejcik, III,¹⁶ R. Vidal,⁷ M. Vondracek,¹⁰ D. Vucinic,¹⁵ R. G. Wagner,¹ R. L. Wagner,⁷ N. Wainer,⁷ R. C. Walker,²⁵ C. Wang,⁶ C. H. Wang,²⁸ G. Wang,²³ J. Wang,⁵ M. J. Wang,²⁸ Q. F. Wang,²⁶ A. Warburton,¹¹ G. Watts,²⁵ T. Watts,²⁷ R. Webb,³⁰ C. Wei,⁶ C. Wendt,³⁴ H. Wenzel,¹⁴ W. C. Wester, III,⁷ T. Westhusing,¹⁰ A. B. Wicklund,¹ E. Wicklund,⁷ R. Wilkinson,²¹ H. H. Williams,²¹ P. Wilson,⁵ B. L. Winer,²⁵ J. Wolinski,³⁰ D. Y. Wu,¹⁶ X. Wu,²³ J. Wyss,²⁰ A. Yagil,⁷ W. Yao,¹⁴ K. Yasuoka,³² Y. Ye,¹¹ G. P. Yeh,⁷ P. Yeh,²⁸ M. Yin,⁶ J. Yoh,⁷ C. Yosef,¹⁷ T. Yoshida,¹⁹ D. Yovanovitch,⁷ I. Yu,³⁵ J. C. Yun,⁷ A. Zanetti,²³ F. Zetti,²³ L. Zhang,³⁴ S. Zhang,¹⁶ W. Zhang,²¹ and S. Zucchelli²

(CDF Collaboration)

¹ Argonne National Laboratory, Argonne, Illinois 60439

² Istituto Nazionale di Fisica Nucleare, University of Bologna, I-40126 Bologna, Italy

³ Brandeis University, Waltham, Massachusetts 02254

⁴ University of California at Los Angeles, Los Angeles, California 90024

⁵ University of Chicago, Chicago, Illinois 60637

⁶ Duke University, Durham, North Carolina 27708

⁷ Fermi National Accelerator Laboratory, Batavia, Illinois 60510

⁸ Laboratori Nazionali di Frascati, Istituto Nazionale di Fisica Nucleare, I-00044 Frascati, Italy

⁹ Harvard University, Cambridge, Massachusetts 02138

¹⁰ University of Illinois, Urbana, Illinois 61801

¹¹ Institute of Particle Physics, McGill University, Montreal H3A 2T8, and University of Toronto, Toronto M5S 1A7, Canada

- ¹² *The Johns Hopkins University, Baltimore, Maryland 21218*
- ¹³ *National Laboratory for High Energy Physics (KEK), Tsukuba, Ibaraki 305, Japan*
- ¹⁴ *Lawrence Berkeley Laboratory, Berkeley, California 94720*
- ¹⁵ *Massachusetts Institute of Technology, Cambridge, Massachusetts 02139*
- ¹⁶ *University of Michigan, Ann Arbor, Michigan 48109*
- ¹⁷ *Michigan State University, East Lansing, Michigan 48824*
- ¹⁸ *University of New Mexico, Albuquerque, New Mexico 87131*
- ¹⁹ *Osaka City University, Osaka 588, Japan*
- ²⁰ *Universita di Padova, Istituto Nazionale di Fisica Nucleare, Sezione di Padova, I-35131 Padova, Italy*
- ²¹ *University of Pennsylvania, Philadelphia, Pennsylvania 19104*
- ²² *University of Pittsburgh, Pittsburgh, Pennsylvania 15260*
- ²³ *Istituto Nazionale di Fisica Nucleare, University and Scuola Normale Superiore of Pisa, I-56100 Pisa, Italy*
- ²⁴ *Purdue University, West Lafayette, Indiana 47907*
- ²⁵ *University of Rochester, Rochester, New York 14627*
- ²⁶ *Rockefeller University, New York, New York 10021*
- ²⁷ *Rutgers University, Piscataway, New Jersey 08854*
- ²⁸ *Academia Sinica, Taiwan 11529, Republic of China*
- ²⁹ *Superconducting Super Collider Laboratory, Dallas, Texas 75237*
- ³⁰ *Texas A&M University, College Station, Texas 77843*
- ³¹ *Texas Tech University, Lubbock, Texas 79409*
- ³² *University of Tsukuba, Tsukuba, Ibaraki 305, Japan*
- ³³ *Tufts University, Medford, Massachusetts 02155*
- ³⁴ *University of Wisconsin, Madison, Wisconsin 53706*
- ³⁵ *Yale University, New Haven, Connecticut 06511*

Abstract

We present a measurement of $\sigma \cdot B(W \rightarrow e\nu)$ and $\sigma \cdot B(Z^0 \rightarrow e^+e^-)$ in proton - antiproton collisions at $\sqrt{s} = 1.8$ TeV using a significantly improved understanding of the integrated luminosity. The data represent an integrated luminosity of 19.7 pb^{-1} from the 1992-1993 run with the Collider Detector at Fermilab (CDF). We find $\sigma \cdot B(W \rightarrow e\nu) = 2.49 \pm 0.12 \text{ nb}$ and $\sigma \cdot B(Z^0 \rightarrow e^+e^-) = 0.231 \pm 0.012 \text{ nb}$.

PACS Numbers: 13.38.-b, 13.60.Hb, 14.70.-e

Measurements of the product of the production cross section and the leptonic branching ratio for W and Z^0 bosons, $\sigma \cdot B(W \rightarrow e\nu)$ and $\sigma \cdot B(Z^0 \rightarrow e^+e^-)$, test the consistency of the standard model couplings [1], the understanding of higher order QCD contributions [2], and the parton distribution functions of the proton. In perturbation theory, the production cross section is predicted to next-to-next-to-leading order (NNLO), with $\approx 20\%$ corrections to the leading order prediction from NLO and additional $\approx 3\%$ corrections at NNLO [2].

In previous measurements at $\sqrt{s} = 1.8$ TeV [3, 4, 5], the accuracy of the comparison to theoretical predictions has been limited by systematic uncertainties in the overall normalization and statistical uncertainties in the event samples. In Reference [6], CDF has presented the measured value of the ratio $\sigma \cdot B(W \rightarrow e\nu)/\sigma \cdot B(Z^0 \rightarrow e^+e^-)$ from the 1992-1993 data, but not the individual cross sections. In References [7, 8, 9], CDF has presented detailed

descriptions of the measurements of the elastic, single diffractive, and total cross sections at $\sqrt{s} = 1.8$ TeV, though not a description of the luminosity normalization. In this Letter, we report new measurements of $\sigma \cdot B(W \rightarrow e\nu)$ and $\sigma \cdot B(Z^0 \rightarrow e^+e^-)$ using our new precise luminosity normalization. Details of the luminosity measurement are included.

CDF [10] combines a solenoidal magnetic spectrometer with electromagnetic (EM) and hadronic (HAD) calorimeters arranged in a projective tower geometry covering the pseudo-rapidity range $|\eta| \leq 4.2$ [11]. Proportional chambers in the EM shower counters provide a measurement of shower position and profile in both the azimuthal (ϕ) and beam (z) directions. Charged particle tracking chambers are immersed in a 1.4 T magnetic field oriented along the beam direction. Forward scintillator planes known as the Beam-Beam Counters, (BBC), covering $3.2 \leq |\eta| \leq 5.9$ and located 5.8 m from the nominal interaction point, serve as the primary luminosity monitor. For the elastic, single diffractive, and total cross section measurements, dedicated runs during the 1988-1989 data-taking period used a magnetic spectrometer [7] and forward wire chamber telescopes [9] in conjunction with the BBC.

For the measurement of $\sigma \cdot B(W \rightarrow e\nu)$ and $\sigma \cdot B(Z^0 \rightarrow e^+e^-)$, W and Z^0 candidate events are selected from a common sample of high transverse energy electrons [6]. The selection requires a well identified electron candidate with transverse energy greater than 20 GeV. The electron is required to come from a primary vertex position within 60 cm of the nominal interaction point along the z direction.

W candidates are chosen from the electron sample with the requirement that electron candidate is well-isolated in the central calorimeter [6] and the missing transverse energy (\cancel{E}_T), defined as the magnitude of the vector sum of transverse energy over all calorimeter towers in the range $|\eta| \leq 3.6$, be greater than 20 GeV. Events which are consistent with the Z^0 selection (described below) are rejected. There are 13796 W candidate events.

Dielectron candidates are chosen from the electron sample with the requirement that the first candidate electron is well isolated in the central calorimeter and that a second isolated well identified candidate electron [6] also be present. From the dielectron sample, a Z^0 sample is chosen with the further requirement that the invariant mass of the two electrons be in the range 66 – 116 GeV/ c^2 . There are 1312 candidate events in the Z^0 sample.

We consider backgrounds in the W sample from the processes $W \rightarrow \tau \rightarrow e$; $Z^0 \rightarrow e^+e^-$, where one electron is not identified; $Z^0 \rightarrow \tau^+\tau^-$, where one τ decays to a electron; mismeasured QCD jet events; and QCD heavy flavor production. The dominant background contribution is from QCD processes, where one jet produces an isolated high p_T electron candidate and the second jet is mismeasured, mimicking \cancel{E}_T . The second largest process is the background from sequential $W \rightarrow \tau \rightarrow e$ decays. The total background to the W sample is 1700 ± 161 events [6].

We consider backgrounds in the Z^0 sample from QCD processes and from the process $Z^0 \rightarrow \tau^+\tau^-$, where both τ 's decay into electrons. The dominant background contribution is from QCD processes. The total background to the Z^0 sample is 21 ± 9 events [6]. A correction of $(+0.5 \pm 0.2)\%$ is applied to the number of Z^0 candidates to account for electron pairs in the mass window from the Drell-Yan γ continuum and electron pairs outside the mass window from the Z^0 [6].

The acceptances, which combine the fiducial and kinematic requirements, are determined from a Monte Carlo program which generates bosons from the lowest order diagram, $q\bar{q} \rightarrow W$ or Z^0 . The bosons are given a transverse momentum (p_T) according to the W p_T distribution previously measured by CDF [12]. The electron and neutrino energies are smeared with the calorimeter energy resolutions. By varying the input parameters to the model, including the parton distribution functions, W mass, detector resolutions and energy scale, and input boson p_T distribution, we estimate systematic uncertainties in the acceptances. Using the MRSD-' [13] parton distribution functions and the world averages [14] of the ElectroWeak parameters, we find the W acceptance to be 0.342 ± 0.008 and the Z^0 acceptance to be 0.409 ± 0.005 [6].

Electron identification efficiencies (including the trigger efficiency) are studied with a sample of Z^0 candidates for which minimal cuts have been imposed on the second lepton. The Z^0 identification efficiency is dependent on the individual electron efficiencies and the angular distribution of the second electron, since the requirements and efficiencies have η dependencies. We find the electron selection for W decays to have an efficiency of 0.754 ± 0.011 and the electron selection for Z^0 decays to have an efficiency of 0.729 ± 0.016 [6].

The requirement that the primary vertex be within 60 cm of the nominal interaction position is chosen to keep the events well contained in the fiducial coverage. The primary vertices have an approximately Gaussian distribution along the beam direction, with $\sigma \approx 26$ cm. To calculate the efficiency of the vertex cut, we model the distribution as a convolution of two Gaussians (the p and \bar{p} distributions) with the accelerator β function [15]. The data are fit over the range ± 60 cm to give a best estimate of the accelerator parameters, which are then used in the calculation of the efficiency. The p and \bar{p} distributions are used as inputs to the calculation on a fill-by-fill basis [16]. We estimate the uncertainty by varying the parameters of the model within their 1σ uncertainties. Weighting the different fills by their respective integrated exposures, we find an efficiency of the vertex cut of 0.955 ± 0.011 .

The W and Z^0 cross sections are normalized to the visible cross section, σ_{BBC} , in the Beam Beam counters [17]. Hits in both planes that arrive coincident with the particle bunches crossing through the detector serve as both a minimum-bias trigger (the BBC trigger) and the primary luminosity monitor. The rate (number) of coincidences in these counters, divided by σ_{BBC} gives the instantaneous (integrated) luminosity. In previous publications, CDF normalized the BBC cross section ($\sigma_{BBC} = 46.8 \pm 3.2$ mb) to UA4 [18] and accelerator measurements at $\sqrt{s} = 546$ GeV, extrapolated to $\sqrt{s} = 1.8$ TeV [3]. With recent direct measurements of the elastic and total cross sections by CDF [7, 9], we are able to make a direct measurement of σ_{BBC} .

The value of σ_{BBC} can be expressed as:

$$\sigma_{BBC} = \sigma_{tot} \cdot \frac{N_{BBC}^{vis}}{N_{inel} + N_{el}} \quad (1)$$

where N_{BBC}^{vis} are the number of BBC triggered events, and N_{inel} and N_{el} are the total number of inelastic and elastic events.

For computational purposes, it is convenient to separate the number of inelastic events into two contributions that have been independently measured, $N_{inel} = N_i + N_d$. N_i is the number of events with a two-sided coincidence in either the BBC or the forward telescopes,

and N_d is the number of events with a single \bar{p} detected in the magnetic spectrometer coincident with hits in the opposite side BBC or forward telescope [9]. We write N_{el} in terms of the parameters of the fit to the elastic scattering data, $N_{el} = A/b$, where $A = dN_{el}/dt|_{t=0}$ is the number of elastic events evaluated where the four-momentum transfer squared, $-t$, equals zero and b is the logarithmic elastic slope parameter [7]. With these definitions and the luminosity independent expression for the total cross section as in Reference [9], σ_{BBC} reduces to:

$$\sigma_{BBC} = \frac{16\pi(\hbar c)^2}{1 + \rho^2} \cdot \frac{N_{BBC}^{vis}}{N_i} \cdot \frac{A}{(A/b + N_i + N_d)^2} \cdot N_i, \quad (2)$$

where ρ is ratio of the real to imaginary part of the forward scattering amplitude. The advantage of this formulation is that most of the quantities are measured independently, simplifying the uncertainty calculations.

Table 1 presents the values used in the calculation of σ_{BBC} . The quantity N_i is a superset of N_{BBC}^{vis} , and includes a Monte Carlo acceptance correction of +1.2%. We find 98.7% of N_i triggered events are BBC triggered events. Therefore, $N_{BBC}^{vis}/N_i = 0.987/1.012 = 0.975$, where we have included the acceptance uncertainty in the uncertainty on N_i (the statistical uncertainty on this quantity is less than 0.1%). We use the measured value of $\rho = 0.140 \pm 0.069$ at $\sqrt{s} = 1.8$ TeV [19] in our calculation. With Table 1, these values, and Equation 2, we calculate $\sigma_{BBC} = 51.15 \pm 1.60$ mb.

In the total cross section measurement [9], we defined a good BBC event to have hits on both sides of the detector, coincident with beam crossing, and required the vertex position reconstructed using timing to be within 3 m of the nominal interaction position. For the integrated luminosity measurement used in $\sigma \cdot B(W \rightarrow e\nu)$ and $\sigma \cdot B(Z^0 \rightarrow e^+e^-)$, we require only that the hits be coincident with the beam crossing. The difference in the event definition has been studied in an unbiased trigger sample, where the only requirement is a beam crossing. The two definitions agree at the level of 0.5%, which is included as a systematic uncertainty for the integrated luminosity calculation.

CDF has made significant changes to the detector since the total cross section measurements, especially in the small angle region (removal of the forward wire chambers and a different beam pipe). Investigations of the vertex distributions, timing information in the BBC's, and the rates in the EM and HAD shower counters show no measurable difference in the BBC cross section within a statistical uncertainty of 1%. Therefore we have included an additional systematic uncertainty of 1.0% in the normalization to account for differences in σ_{BBC} due to uncertainties in the detector acceptance.

The accelerator running conditions during the data taking were also significantly different from those during the total cross section measurements. The average instantaneous luminosity during the data taking was $3.5 \times 10^{30} \text{ cm}^{-2} \text{ sec}^{-1}$, in contrast to $10^{28} \text{ cm}^{-2} \text{ sec}^{-1}$ during the total cross section measurement. Accidental coincidences in the BBC's (from overlapping single diffractive events and machine losses, for example) have been studied in detail. We apply an average correction of $(-1.3 \pm 1.0)\%$ to the integrated luminosity. We have also investigated the effects of backgrounds which give real coincidences (e.g., beam - gas interactions) and include a 1% uncertainty as an upper limit on the magnitude of these backgrounds. Combining the measurement uncertainty with the acceptance and correction

	Number of events
N_i	208890 ± 2558
N_d	32092 ± 1503
N_{el}	78691 ± 1463
$A \, dN_{el}/dt _{t=0}$	$1336532 \pm 40943 \text{ (GeV}^{-2}\text{)}$
$b \text{ Elastic Slope}$	$16.98 \pm 0.25 \text{ (GeV}^{-2}\text{)}$
$\text{Covariance}(A, b)$	0.93

Table 1: Summary of results from the total cross section measurement used in the calculation of σ_{BBC} (from Reference [7,9]). The $\text{Covariance}(A, b)$ is the correlation coefficient in the 2 dimensional fit to the elastic slope and $dN_{el}/dt|_{t=0}$.

uncertainties gives a total uncertainty of 3.6% in the integrated luminosity, a substantial improvement over the 6.8% reported previously [3]. The data set for the W and Z^0 analyses has an integrated luminosity of $19.7 \pm 0.7 \text{ pb}^{-1}$.

Combining the event samples, backgrounds, acceptances, efficiencies and integrated luminosities shown in Table 2, we find $\sigma \cdot B(W \rightarrow e\nu) = 2.49 \pm 0.02 \text{ (stat)} \pm 0.08 \text{ (syst)} \pm 0.09 \text{ (lum) nb}$ and $\sigma \cdot B(Z^0 \rightarrow e^+e^-) = 0.231 \pm 0.006 \text{ (stat)} \pm 0.007 \text{ (syst)} \pm 0.008 \text{ (lum) nb}$. In Figure 1, we compare these cross section values to theoretical predictions, along with measurements at $\sqrt{s} = 630 \text{ GeV}$ from the UA1 [20] and UA2 [21] collaborations and $\sqrt{s} = 1.8 \text{ TeV}$ from the D0 [22] collaboration.

In the insets to Figure 1, we show the variation in the predicted cross section times branching ratio for different sets of parton distribution functions [2, 23, 24], compared to the current CDF measurement. For the W case, the total uncertainty is 4.9% and is consistent with all sets, though consistently larger than the predictions. A recent analysis [23] of parton distribution functions shows that the evolution of the u and d distributions from $Q^2 \approx 20 \text{ GeV}^2$ (as measured in fixed target data) to $Q^2 \approx M_W^2$ (which determines the W production cross section) depends appreciably on the gluon distribution with $x \approx 0.05$. In this x range, the gluon distribution is currently not well constrained [23] and further measurements of the W and Z production cross sections could provide additional information for the parton distribution functions.

In summary, we have presented measurements of $\sigma \cdot B(W \rightarrow e\nu)$ and $\sigma \cdot B(Z^0 \rightarrow e^+e^-)$, including a precise luminosity normalization calculation. The measurements are in good agreement with NNLO theoretical predictions. We foresee using the $\sigma \cdot B(W \rightarrow e\nu)$ measurement as the determination of the collider luminosity in future Tevatron runs.

We thank the Fermilab staff and the technical staffs of the participating institutions for their vital contributions. We thank James Stirling for advice. This work was supported by the U.S. Department of Energy and National Science Foundation; the Italian Istituto Nazionale di Fisica Nucleare; the Ministry of Education, Science and Culture of Japan; the Natural Sciences and Engineering Research Council of Canada; the National Science Council of the Republic of China; and the A. P. Sloan Foundation.

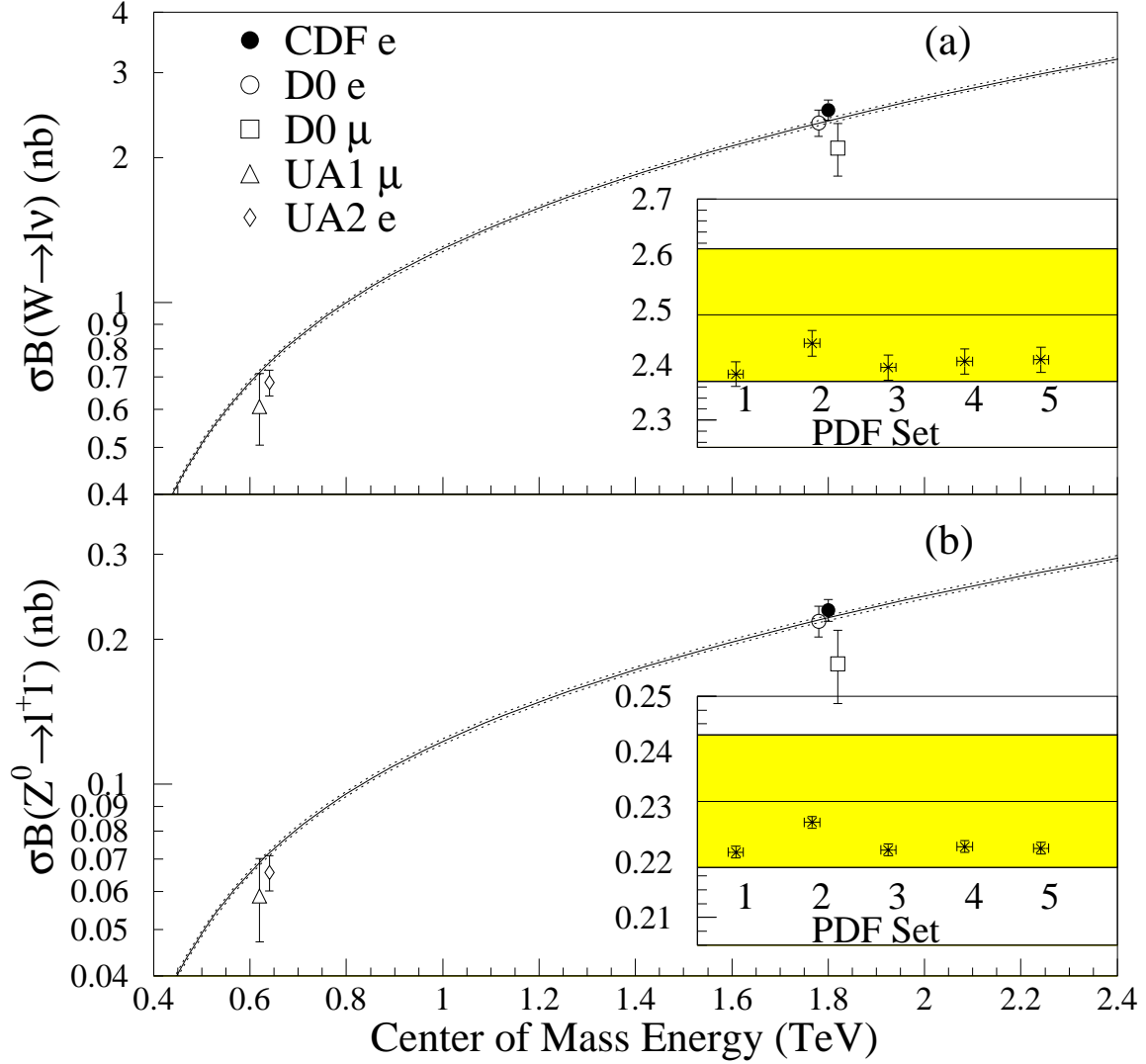


Figure 1: Comparison of measured (a) $\sigma \cdot B(W \rightarrow e\nu)$ and (b) $\sigma \cdot B(Z^0 \rightarrow e^+e^-)$ to theoretical predictions using the calculation from Reference [2] and MRSA [23] parton distribution functions. The UA1 and UA2 measurements and D0 measurements are offset horizontally by ± 0.02 TeV for clarity. In the inset, the shaded area shows the 1σ region of the CDF measurement; the stars show the predictions using various parton distribution function sets (1) MRSA, (2) MRSD0', (3) MRSD-', (4) MRSH [23] and (5) CTEQ2M [24]. The theoretical points include a common uncertainty in the predictions from choice of renormalization scale ($M_W/2$ to $2M_W$).

	W Events	Z^0 Events
Candidates	13796	1312
Total Background	1700 ± 161	21 ± 9
Signal	$12096 \pm 117 \pm 161$	$1291 \pm 36 \pm 9$
Drell-Yan Correction	–	1.005 ± 0.002
Acceptance	0.342 ± 0.008	0.409 ± 0.005
Efficiency	0.754 ± 0.011	0.729 ± 0.016
Vertex Efficiency	0.955 ± 0.011	0.955 ± 0.011
Luminosity	$19.7 \pm 0.7 \text{ pb}^{-1}$	$19.7 \pm 0.7 \text{ pb}^{-1}$
Cross Sections	2.49 ± 0.02 (stat) ± 0.08 (syst) ± 0.09 (lum) nb	0.231 ± 0.006 (stat) ± 0.007 (syst) ± 0.008 (lum) nb

Table 2: Summary of results on $\sigma \cdot B(W \rightarrow e\nu)$ and $\sigma \cdot B(Z^0 \rightarrow e^+e^-)$.

References

- [1] S.L. Glashow, Nucl. Phys. **22**, 579 (1961); S. Weinberg, Phys. Rev. Lett. **19** 1264 (1967); A. Salam, in *Elementary Particle Physics: Relativistic Groups and Analyticity (Nobel Symposium No. 8)*, edited by N. Svartholm (Almqvist and Wiksell, Stockholm, 1968), p. 367.
- [2] R. Hamberg, T. Matsuura, and W.L. van Neerven, Nucl. Phys. **B345**, 331 (1990); Nucl. Phys. **B359**, 343 (1991); W.L. van Neerven and E.B. Zijlstra, Nucl. Phys. **B382**, 11 (1992).
- [3] F. Abe, *et al.*, Phys. Rev. **D 44**, 29 (1991).
- [4] F. Abe, *et al.*, Phys. Rev. Lett. **68**, 3398 (1992).
- [5] F. Abe, *et al.*, Phys. Rev. Lett. **69**, 28 (1992).
- [6] F. Abe, *et al.*, Phys. Rev. Lett. **73**, 220 (1994). F. Abe, *et al.*, Phys. Rev. **D52**, 2624 (1995).
- [7] F. Abe, *et al.*, Phys. Rev. **D 50**, 5518 (1994).
- [8] F. Abe, *et al.*, Phys. Rev. **D 50**, 5535 (1994).
- [9] F. Abe, *et al.*, Phys. Rev. **D 50**, 5550 (1994).
- [10] F. Abe, *et al.*, Nucl. Instr. Meth. **A271**, 387 (1988) and references therein.
- [11] The CDF coordinate system defines z along the proton-beam direction, θ as the polar angle, and ϕ as the azimuthal angle. The pseudo-rapidity is defined as $\eta = -\ln(\tan(\theta/2))$.
- [12] F. Abe, *et al.*, Phys. Rev. Lett. **66**, 2951 (1991).

- [13] A.D. Martin, R.G. Roberts, and W.J. Stirling, Phys. Lett. **B 306**, 145 (1993); Phys. Lett. **B 309**, 429E (1993).
- [14] LEP ElectroWeak working group, CERN report No. CERN/PPE/93-157, 26 August 1993.
- [15] M. Conte and W. MacKay, *An Introduction to the Physics of Particle Accelerators*, (World Scientific, Singapore, 1991), p. 76.
- [16] The Tevatron is filled with p and \bar{p} beams approximately once per day and each fill has slightly different properties.
- [17] We wish to emphasize that this normalization is a visible cross section, dependent upon the secondary interactions, photon conversions, etc., which take place in the material between the interaction region and the BBC's.
- [18] M. Bozzo, *et al.*, Phys. Lett. **147B**, 392 (1984).
- [19] N. Amos, *et al.*, Phys. Rev. Lett. **68**, 2433 (1992).
- [20] C. Albajar, *et al.*, Phys. Lett. **B 253**, 503 (1991).
- [21] J. Alitti, *et al.*, Z. Phys. C **47**, 11 (1990).
- [22] S. Abachi, *et al.*, Phys. Rev. Lett. **75**, 1456 (1995).
- [23] A.D. Martin, W.J. Stirling, and R.G. Roberts, preprint RAL-94-055 and DTP/94/34 (1994) and references therein.
- [24] Wu-Ki Tung, in *Proceedings of International Workshop on Deep Inelastic Scattering and Related Subjects*, Eilat, Israel, 1994 World Sci., Singapore.